**Please answer all sections of the document. You are welcome to use figures and tables to complement or enhance the text. For annual reports, please only describe work for the period of performance (July 1, 2013 - June 30, 2014). For final reports, please describe the comprehensive effort.**

**Grant/Award #: IACRO 13-5897I (previous id's: 12-2026I, 11-4471I, 10-4257I)**
**PI Name: David P. Adams**
**Organization/Institution: Sandia National Laboratories**
**Project Title: Basic Research of Intrinsic, Tamper Indication Markings and Patterns Defined by Pulsed Laser Irradiation**

**What are the major goals of the project?**
*List the major goals of the project as stated in the approved application or as approved by the agency. If the application lists milestones/target dates for important activities or phases of the project, identify these dates and show actual completion dates or the percentage of completion. Generally, the goals will not change from one reporting period to the next. However, if the awarding agency approved changes to the goals during the reporting period, list the revised goals and objectives. Also explain any significant changes in approach or methods from the agency-approved application or plan.*

The goals of this project for the past 12 months were:

Task 2: Research of laser-induced periodic surface structures

Sub-task 2.4 Investigate the roles of surface plasmon polaritons (SPP) and the effects of fluence on laser-induced periodic surface structures.

Sub-task 2.5 Using an Electromagnetic (EM) solver, model the light-solid interactions that give rise to laser-induced period surface structures.

Task 6: Research the stability of color layers and laser-induced periodic surface structures

Sub-task 6.1 Investigate the corrosion resistance of color layers using salt fog, salt spray, and salt immersion testing.

Task 7: Research methods of feature interrogation

Sub-task 7.1 Investigate light-based methods for inspection and validation of markings This will include non-invasive, non contact methods for locating and identifying localized color features created by nanosecond pulsed laser irradiation.

Note: these tasks were also specified in the 2013 year end report for this research project.

*Sandia is a multi-program laboratory managed and operated by Sandia Corporation, a wholly owned subsidiary of Lockheed Martin Company, for the United States Department of Energy's National Nuclear Security Administration under Contract DE-AC04-94AL85000.*

**What was accomplished under these goals?**
*For this reporting period describe: 1) major activities; 2) specific objectives; 3) significant results, including major findings, developments, or conclusions (both positive and negative); and 4) key outcomes or other achievements. Include a discussion of stated goals not met. As the project progresses, the emphasis in reporting in this section should shift from reporting activities to reporting accomplishments.*

Research of laser-induced periodic surface structures (Task 2)

*Major Activities*

With our previous research, it was found that surface asperities or roughness must be present to create periodic surface structures upon laser exposure. In particular, an initial rough surface morphology (such as that found with a machined surface) provides multiple sites for light scattering, which underlies the formation of periodic ripple morphologies. Light scattering from a random surface creates patterns of periodic structures (with complex orientations) that could be used as intrinsic markings for tagging materials and equipment. Despite these initial findings, the fundamental mechanisms that give rise to periodic surface structures and their characteristic shapes were not identified in prior research.

Toward this end, our work in the past year has investigated the fundamental physics underlying the formation of laser-induced periodic surface structures (LIPSS). A combination of experiments and numeric modeling has identified several light-solid interactions that are responsible for surface structure formation. With this information, one should be able to predict the general characteristics of surface morphologies and what materials form periodic ripples.

*Specific Objectives*

The two specific objectives for the previous year were as follows.

- Investigate the roles of surface plasmon polaritons (SPP) and the effects of fluence on laser-induced periodic surface structures. (Sub-task 2.4)
- Using an Electromagnetic (EM) solver, model the light-solid interactions that give rise to laser-induced period surface structures. (Sub-task 2.5)

*Significant Results and Findings*

Our research has identified surface plasmon polariton excitation and Fresnel diffraction as being responsible for the formation of periodic surface structures during single-pulse femtosecond irradiation. Furthermore, the relative contributions of these two light-solid interactions vary as a function of the light polarization direction. Experiments that determine the contributions of these light-solid interactions have involved irradiating stepped, 110 nm-high Au microstructures fabricated on Si substrates. Microstructures with straight edges were chosen, because these allow for alignment (and deliberate mis-alignment) of the laser polarization vector with respect to well-defined linear step-edges. By varying the laser polarization vector orientation between experiments, we access regimes wherein SPP excitation should be active, and other cases in which SPP excitation is minimized and Fresnel diffraction can dominate.

For experimental tests, a Clark-MXR CPA-2001 Ti:sapphire pulsed laser with a 150 fs pulse length, centered near a wavelength of 780 nm, with a repetition rate of 1 kHz, a maximum pulse energy of 1 mJ, and a Gaussian intensity profile, was focused to a 1/e2 diameter of 40 μm using a 20 cm focal length lens and directed toward a specimen at normal incidence. Samples were affixed within the focus of the beam using a Newport 4-axis translation stage, which allows for positioning in the x, y, and z lab directions with 2 μm accuracy. All irradiation experiments were conducted in air, and the focus of the laser beam was centered on mesa edges. Experiments have varied laser fluence (J/cm$^2$) independent of laser polarization direction to study the effects of increasing energy on target. Single laser pulses were used for irradiation.

Starting with a high laser fluence (0.64 J/cm$^2$), we observe the formation of periodic structures when irradiating an edge of a square mesa. Results shown in Fig. 1 are taken after a single, linearly polarized laser pulse was directed at the sample surface. Evident in Fig. 1(a), LIPSS form on both the Au film (gold color) and Si substrate (blue color) with wavevectors perpendicular to the mesa step-edge when the laser polarization vector is perpendicular to the edge. In Fig. 1(b), a different structure type is found when the laser polarization vector is parallel to the microfabricated edge. LIPSS are visible on the Au and Si surfaces with wavevectors both perpendicular and parallel to the step-edge and at other orientations when the laser polarization vector is parallel to the edge.

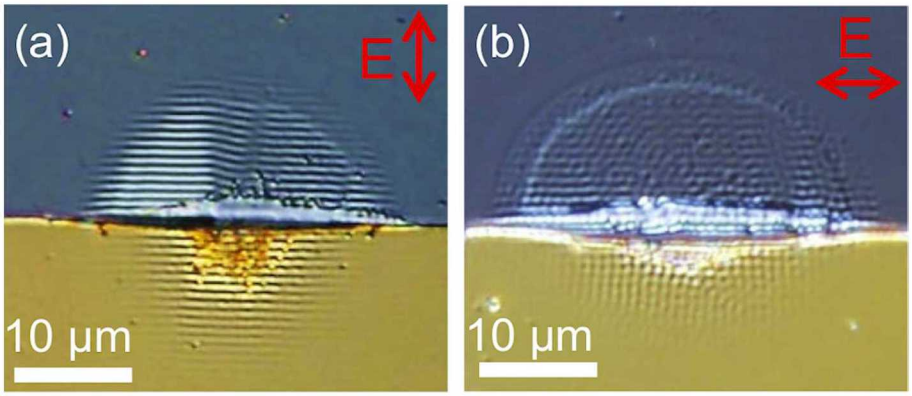


FIG. 1. LIPSS formation on Au and Si surfaces after irradiation of a mesa edge at a high fluence of 0.64 J/cm$^2$. (a) When the laser polarization vector is perpendicular to the edge, LIPSS mostly form with wavevectors perpendicular to the edge. (b) When the laser polarization vector is parallel to the edge, LIPSS form with wavevectors both perpendicular and parallel to the edge and at other orientations.

Periodic surface ripples also form when exposing surfaces to a reduced fluence, although interesting differences are observed. The effects of irradiating one edge of a square mesa edge with a single, linearly polarized laser pulse at a fluence of 0.30 J/cm$^2$ are shown in Fig. 2. LIPSS formation on the Si surface is readily apparent for both polarizations. Periodic structures are present on the Au surfaces in Figs. 2(a) and 2(b), although not easily recognized in these optical microscope images. Atomic force microscopy (AFM) measurements of surface height taken perpendicular to mesa edges show that the LIPSS formed on Si are a series of peaks above and valleys below the original Si surface. AFM height traces, taken perpendicular to mesa edges from Figs. 2(a) and 2(b), show that LIPSS valleys below the original Si surface have larger amplitudes than those of neighboring peaks that lie above the original surface, suggesting net mass loss. LIPSS created by light that has a polarization vector oriented perpendicular to mesa edges have average peak-to-peak amplitudes which are larger than the amplitudes of structures created using a polarization vector that is parallel to mesa edges.

AFM traces were obtained from at least 30 different regions where LIPSS formed, and periodicity distributions within the irradiated Si regions were determined by performing Fourier transforms of AFM height traces of individual LIPSS features. The resulting distributions of periods are graphed in the bottom of Fig. 2 to show the effects of incident light polarization. When the laser polarization vector is perpendicular to a mesa edge, LIPSS mostly form with

wavevectors perpendicular to the edge. A distribution of periods peaked near a value of 710 nm results, which is less than the incident light wavelength. Important to the complexity of produced laser markings, we find that the periodicity of surface structures shift to even lower values with increased fluence, consistent with the even smaller periodicity of features shown in Fig. 1 for a fluence of 0.64 J/cm$^2$. For laser polarization vectors parallel to mesa edges, as in Fig. 2(b), LIPSS form on Si surfaces with wavevectors both perpendicular to the mesa edge and at other orientations. In this case, the distribution of periods measured in directions perpendicular to the mesa edge is not peaked near a single wavelength.

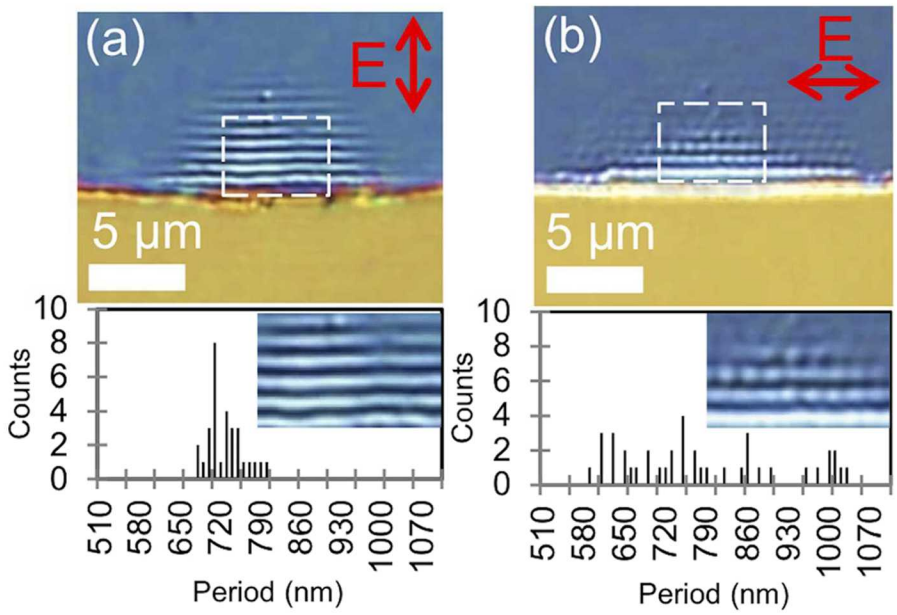


FIG. 2. Optical images obtained after irradiation of a mesa edge at a fluence of 0.30 J/cm$^2$ for two different laser polarizations. The histogram plots below each image show the distributions of LIPSS periods on the Si surface for each laser polarization, measured in a direction perpendicular to the mesa edge. (a) When the laser polarization vector is perpendicular to the mesa edge, the distribution of measured LIPSS periods is peaked near a single value. (b) When the laser polarization vector is parallel to the mesa edge, the distribution of periods is not peaked near a particular value.

Irradiation of a mesa edge at a low fluence of 0.20 J/cm$^2$ (which corresponds to the threshold for melting bulk Si substrates) resulted in subtle periodic structures. For laser polarization vectors that are perpendicular to mesa edges, periodic structures are detected. As seen in Fig. 3(a) ,

periodic structures are present a few microns from the mesa step edge on both Au and Si. AFM measurements of the periodic structures on the Si surface, however, did not detect height changes, yet some compositional modulation is suggested by optical microscopy. Slight changes to height (of the order of 1-2 nm) were detected in the irradiated gold. For laser polarization vectors parallel to mesa edges, irradiation at 0.20 J/cm$^2$ produced no detectable periodic structures on either the Au or Si surfaces. Below 0.20 J/cm$^2$, no periodic structures were observed on either the Au film or Si substrate for any in-plane orientation of the laser polarization vector.

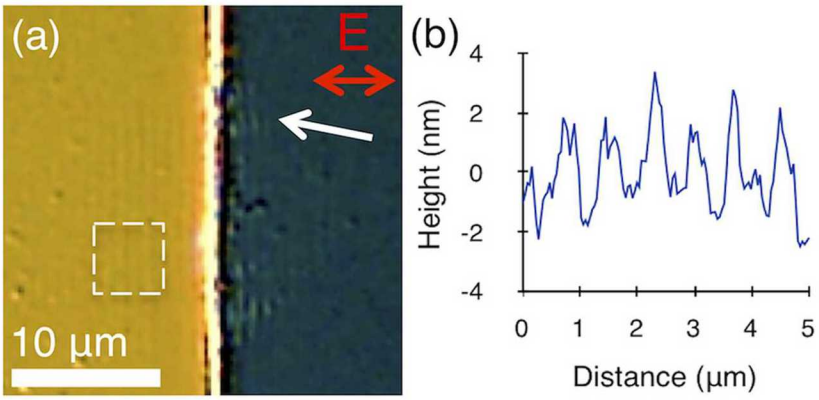


FIG. 3. (a) DIC image of periodic structure formation on Au and Si surfaces after irradiation by a single laser pulse at a fluence of 0.20 J/cm$^2$. The laser polarization vector was perpendicular to the mesa edge. The single arrow indicates periodic structures on the Si surface. (b) Average height trace from the Au region outlined in Fig. 3(a). The trace shows periodic valleys and hills on the Au surface. Height 0 corresponds to the original Au surface.

One can expect that the periodic spatial distribution of light at a material surface gives rise to the periodic surface structures through variations in the local surface temperatures. Material can be flowed, evaporated, or ablated from select regions that are exposed to high intensity fields to produce the final surface morphology. Depending on the irradiation conditions, diffraction of laser light from surface features and SPP excitation during irradiation are expected to participate in this process by changing the local intensity and frequency of light which is coupled to the irradiated surface. SPP excitation is known to be a polarization dependent process which increases the local intensity of light at metallic surfaces, and Si surfaces irradiated by high-intensity laser light, when a component of the laser polarization is perpendicular to surface

defects. Specifically, the excitation of SPPs is predicted to increase the intensity of light at the surface and shift the wavelength of coupled light below that of the incident light, consistent with measurements described above. When the laser polarization vector is parallel to edges, SPP excitation is minimized, and we expect that Fresnel diffraction dominates.

In this study, mesa edges are surface defects, which should, in turn, excite SPPs during laser irradiation. When the laser polarization vector is perpendicular to an edge, it was found for fluences 0.64 J/cm$^2$ and 0.30 J/cm$^2$ that the amplitude of LIPSS valleys and hills on the Si surfaces were greater than when the polarization vector was parallel to edges. This is consistent with amplified field intensity at localized, periodic sites. Also, LIPSS wavevectors were perpendicular to a mesa edge when the laser polarization vector is perpendicular to that edge, and in Fig. 2(a), the LIPSS period is peaked near a single value that is well below that of the fundamental wavelength. Based on these observations, we conclude that SPP excitation plays a significant role in LIPSS formation when a component of the laser polarization vector is perpendicular to mesa edges.

When SPP excitation is minimized (through control of polarization), LIPSS are still observed but in multiple orientations. LIPSS are not, however, regular which means that the period is not well defined or centered near a particular periodicity as when SPP excitation is dominant. Knowing that SPP excitation is at least minimized in this case, we expect that the previously identified Fresnel diffraction of light scattered from step edges plays a role in LIPSS formation when polarization is set parallel to step edges.

With regard to fabricating markings that protect against counterfeiting and related activities, these results suggest how complex patterns will be formed on component surfaces. Component surfaces are microscopically rough and characterized by a plethora of light scattering sites with different edge orientations. Scanning a laser beam of fixed polarization across such a surface would access a variety of different polarization – edge orientations and these will lead to a complex mixture of ripple patterns that vary in space. Specifically, the period and amplitude of local surface structures will vary as surface plasmons will be excited in some regions, but not others. A different strategy that adds complexity to markings would involve changing the power as the beam is scanned across a surface. This also would excite SPPs to different levels and

produce areas of different periodicity with different wavevectors. The microscopic variations of surface structures is envisioned to be information that could be recorded at the time of manufacture and used at the time of inspection and/or validation.

Sub-task 2.5: Using an Electromagnetic (EM) solver, model the light-solid interactions that give rise to laser-induced period surface structures

In the past year, we have initiated a program to model the interaction of ultrashort laser pulses with initially rough surfaces in order to better understand the formation of laser-induced periodic surface structures (LIPSS). This has allowed us to couple our modeling effort with our ongoing experimental studies to better understand the relevant phenomena, and it gives us the ability to predict the outcome of future experiments, as well as, select the laser process parameters to optimize and customize the desired randomized response. The ultrafast laser light-surface coupling simulations were performed using COMSOL, a commercially available software package. The laser-materials interaction problem is included in COMSOL by solving Maxwell's equations employing the finite element method. This gives us the flexibility to include multiple materials on a size scale relevant to the dimensions of our experiments.

Our initial model studies demonstrate that the laser polarization plays a fundamental role in the near-field response of an electromagnetic wave with a stepped feature. Figure 4 shows simulation results for the interaction with the laser field polarized parallel to a Au mesa edge (z-direction) similar to one set of experiments. In this configuration, Fresnel diffraction dominates, since surface plasmon polaritons (SPP) are not allowed by symmetry. The diffracted light leads to a periodic field distribution on the silicon surface, which results in inhomogeneous absorption which can lead to ripple formation when material is selectively removed by ablation, evaporation, etc.

To gain further insight into the role of near-field diffraction at a stepped edge, we performed simulations with mesas of height larger than our 110 nm experimental targets with the goal of

effectively decoupling the Au surface to the substrate. Also evident in Fig. 4, the increased mesa height results in an electromagnetic field on the substrate that is increased in amplitude and shifted in phase. Simulations predict a larger amplitude and shift in the frequency of the ripple structures for increased mesa height when treated with identical fluence (a subject of current experimental validation). The simulations also show no apparent periodic field distribution on the gold surface, consistent with experiments at moderate fluence (Fig. 3). This implies that SPP are the dominant mechanism involved in LIPSS formation at the gold surface.

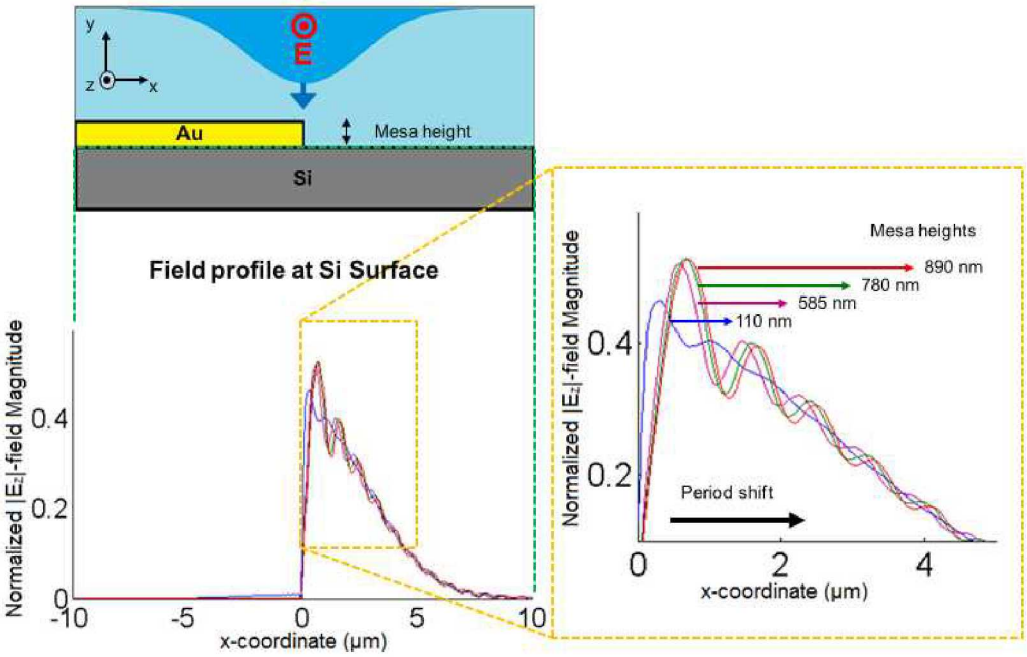


Figure 4. Simulations of the laser interactions with Au mesas of height 110 nm, 585 nm, 790 nm, and 890 nm reveal changes in both the amplitude and phase of the field in the Si substrate depending on mesa height. The polarization of the E-field is parallel to the gold mesa edge in the z direction. In this configuration the LIPSS formation is dominated by Fresnel diffraction. The incident laser wavelength is 780 nm.

Furthermore, to investigate the role of surface plasmon coupling with the electromagnetic field, we performed simulations with the laser polarization perpendicular to the mesa edge as shown in Fig. 5. For this geometry, SPP excitation is found to be dependent on mesa height, and interestingly, the second harmonic of the 780 nm laser field is also observed in the produced

electric field variations. Note: LIPPS at both the fundamental and second harmonic frequency were observed in our experiments on 110 nm Au mesas. We currently believe that the origin of the second harmonic is from reflection of the SPP traveling in the x-direction from the opposite Au mesas edge creating a standing wave pattern. We are, as yet, unsure of the mechanism for the changes in the SPP amplitude due to mesa height. Current experiments include a new round of tests coupled with the modeling effort to investigate the SPP formation dependence on mesa height along with the high harmonic generation observed. Lastly, SPP can be launched in the silicon substrate if the critical electron density is reached. We are currently incorporating this mechanism into our model for future simulations.

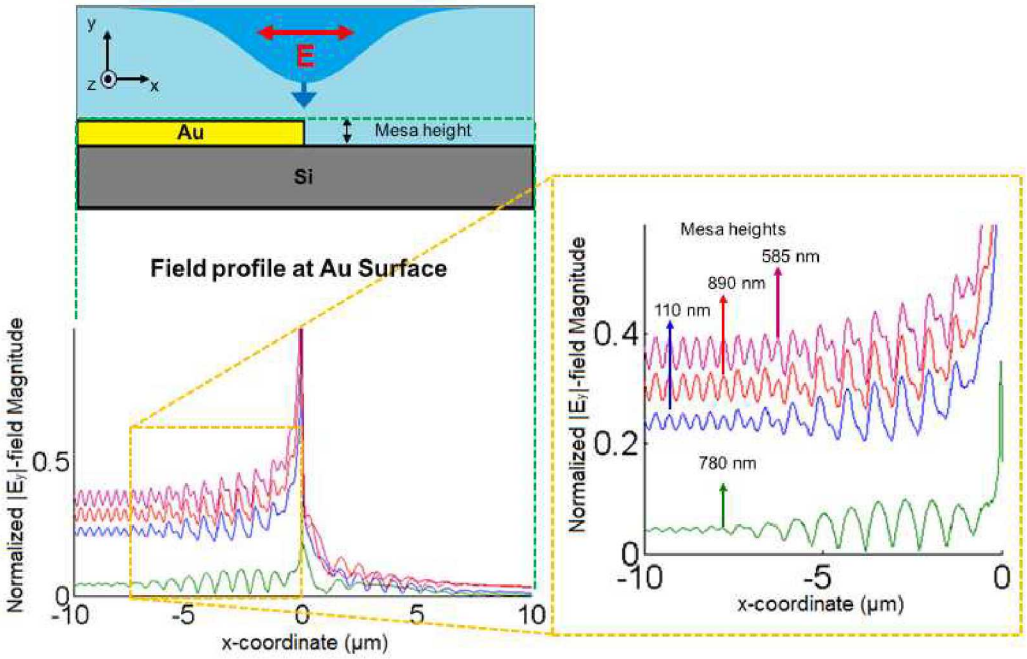


Figure 5. Simulations of the laser interactions with a Au mesa on Si substrate with the polarization of the E-field perpendicular to the gold mesa edge. In this configuration the LIPSS formation is dominated by surface plasmon excitation. The incident laser wavelength is 780 nm. Results are shown for different mesa heights.

The model simulations have served two important functions. First, these have confirmed initial speculation that surface plasmon polaritons and Fresnel diffraction play a role in the production of periodic surface structures and that their relative contributions depend on incident polarization

direction. Second, the model simulations show an additional form of randomness in laser ripple markings. The simulations of light interacting with different mesa heights indicate a variable period in the produced electric field variations. Thus, a relatively-simple, scanned laser process operating with a constant fluence and a constant polarization should produce a variety of local periodic structures with different periodicities. The periodicities should vary according to the initial differences in surface asperity height.

*Key Outcomes*

The key outcomes of this task were the following:

- We have discovered that laser induced periodic surface structure formation is due to the combined effects of Fresnel diffraction and surface plasmon polariton excitation.
- The period and distribution of periods of laser-induced surface structures is affected by both the fluence and polarization direction.
- Initial computer modeling with a commercial electromagnetic solver (COMSOL) has been used to predict the characteristics of electric field variations on surfaces that occur during laser irradiation of stepped surface.
- The predicted electric field characteristics (such as spacing between repeated maxima and amplitude variation away from a step edge) are similar to measured characteristics of laser induced periodic surface structures produced in the laboratory.
- The model predictions predict that the amplitude and period of produced surface structures will vary according to the initial height of asperities present on the starting surface.

Research the stability of color layers and laser induced periodic surface structures (Task 6)

*Major Activities*

In the previous 12 months of research, we have built on initial tests by exploring the corrosion resistance of two material sets (oxides produced on stainless 304L and oxides produced on a Ti alloy, Ti6Al4V). Samples were subjected to extreme corrosion environments involving extended immersion in concentrated salt water as well as less harsh corrosion environments involving salt spray / salt fog. In the latter tests, samples were tested in accordance with the ASTM B117 standard for more than 100 hours each. The effects of corrosion were evaluated by mass change and changes to surface color, phase, and chemistry.

We have discovered that many produced oxide color markings are resistant to corrosion attack. Generally, these are oxide coatings that are not cracked. These particular coatings are made with thicknesses less than ~200 nm (for stainless steel substrates). The corrosion resistance was evaluated and understood in the context of phases formed during laser irradiation and their propensity to form cracks during laser exposure.

*Specific Objectives*

The specific objective for the previous year was specified as:

- Investigate the corrosion resistance of color layers using salt fog, salt spray and salt immersion testing. (Sub-task 6.1)

*Significant Results and Findings*

Sixteen different types of oxide coatings were fabricated on stainless steel 304L substrates for subsequent salt water immersion testing. These were made by adjusting the laser scan rate, and,

hence, the accumulated fluence to produce different oxide thicknesses. Each produced sample was then exposed to an aggressive simulated seawater environment by immersion.

After 48 hours exposure a corrosion product had begun to deposit on the majority of the oxides. Only a few specimens, the 225 kHz/175 mm/s, the 350 kHz/60 mm/s, and the 350 kHz/70 mm/s oxides, were free of any visible corrosion product. After 25 days exposure, a thick, uniform corrosion product covered all oxide areas. Scanning electron microscopy (SEM) imaging revealed that a pervasive corrosion product deposited on top of the laser-oxide coatings and indicated that corrosion was not a result of degradation of the laser-oxide coating itself but rather undercutting by attack of Cr-depleted regions beneath oxide coatings. Additionally, the corrosion product was not well-adhered to the oxide, flaking off easily when handled or imaged with a high energy electron beam. Coupled with low angle X-ray diffraction which indicates the corrosion product is an iron chloride hydrate, it is likely that the product is formed as a result of stainless steel corrosion rather than laser-oxide layer degradation.

Twelve additional oxide coatings were next made on stainless steel 304L coupons for testing in less harsh (but more likely applicable) corrosive environments. As summarized in Table 1, test samples were made by varying the laser-scan velocity with the average laser power fixed at 5.6 W and pulse frequency set to 225 kHz. This resulted in a range of oxide coating thicknesses. Samples were then exposed to a salt spray test conforming to the ASTM B117 standard for more than 100 hours each.

An assessment of the severity of corrosion as a function of oxide thickness reveals that thick coatings (> 200 nm) are susceptible to chlorine attack while oxides of < 200 nm thickness are protective. Micrographs for four of the twelve oxides are presented in Fig. 6.

**Table I.** Laser processing conditions and resulting coating thicknesses for oxide samples subject to salt spray testing. All oxides were fabricated on stainless steel using an average laser power of 5.6 W and a laser pulse frequency of 225 kHz. Pulse duration was 120 ns.

| *Laser Scan Rate (mm/s)* | *Measured Coating Thickness (nm)* |
|---|---|
| 30 | 489 |
| 47 | 405 |
| 80 | 403 |
| 175 | 302 |
| 200 | 285 |
| 225 | 196 |
| 250 | 150 |
| 300 | 147 |
| 350 | 100 |
| 400 | 84 |
| 450 | 65 |
| 500 | 40 |

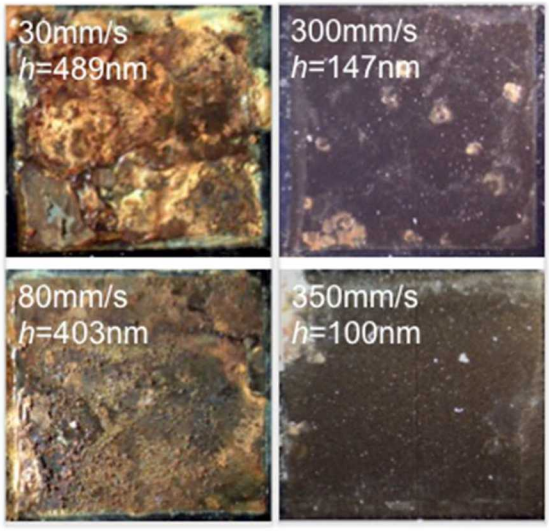


Figure 6: Optical micrographs of six oxide coatings subjected to 168 hours of salt spray exposure. Surface characterization indicates that oxides having a thickness (h) greater than approximately 200 nm are corroded. Coatings with thickness < 200 nm remain intact, to a large degree. This is evidenced with the two samples shown on the right by their original color and lack of corrosion product.

Characterization of these samples and others subjected to salt spray conditions demonstrated that oxides with thicknesses greater than ~200 nm suffer from pervasive through-thickness cracking, which develops as a means to relieve residual stresses in the film resulting from high temperature

laser processing and thermal expansion coefficient differences between the substrate and coating. Through-thickness cracks provide a path for exposure of the substrate immediately beneath the oxide to the aggressive environment. The Cr-depleted SS 304L substrate is susceptible to chloride attack and thus a thick, uniform corrosion product deposits on top of the exposed area. Conversely, oxides with thickness less than ~ 200 nm have no visible surface channel cracking after laser fabrication, suggesting the films are thin enough to avoid significant residual stresses and thus deform in union with the stainless steel substrate. These thin oxides, with a likely mixture of $MnCr_2O_4$ and $Fe_2O_3$, serve as a protective barrier preventing corrosion of the Cr-depleted substrate near interfacial volume.

Based on these findings, we have devised a set of experiments to access thicker, crack-free oxide coatings. Speculating that the larger thermal excursions associated with high fluence (low scan speed) processes give rise to cracks in oxide coatings, we propose future research of methods that maintain a low average fluence per scan. Keeping the fluence low and repeating exposure by making multiple scans over patterned areas, there is a possibility of growing thicker coatings without attaining the high temperatures associated with single scan, high fluence processes.

*Key Outcomes*

The key outcomes of this task are as follows,

- Salt water immersion testing has been completed to assess the corrosion resistance of oxide color markings made on different metal alloy substrates. Extended immersion in concentrated salt water solution led to corrosion attack of oxides made on stainless steel 304L samples.
- Spray corrosion testing has been completed on laser-fabricated oxide markings made on stainless steel 304L and titanium alloy substrates in accordance with the ASTM B117 standard. Tests indicate good corrosion resistance when laser-fabricated oxide coatings are not cracked.

- Colored oxide coatings produced on stainless steel 304L with layer thicknesses less than approximately 200 nm are protective in aggressive chloride environments. These films are thinner than the critical thickness at which surface cracking develops.

- Oxide coatings produced on stainless steel 304L with thicknesses greater than 200 nm suffer from pervasive through-thickness cracking which provide a path for exposure of the stainless steel substrate to the environment. Current laser processing causes Cr diffusion from the substrate to the oxide coating leaving a Cr-denuded zone that extends to about half of the melt zone depth; this Cr-depleted volume is susceptible to corrosion in severe chloride environments.

Research methods of feature interrogation (Task 7)

*Major Activities*

In the past year we have investigated two non-contact, light-based methods for interrogating and validating laser-produced markings. This includes laser speckle analysis, which can potentially be used for remote standoff inspection at distances of the order 1 – 3 m. Second, we have investigated UV-Vis-IR microspectrophotometry as a method for interrogating randomly-placed microscopic color islands contained inside macroscale markings. This commercially available instrument (CRAIC, Inc.) utilizes a modified optical microscope to resolve the microscopic variations in spectral reflectance over large areas. We are currently investigating the spatial and spectroscopic resolution of this approach.

*Specific Objectives*

The specific objective for the previous year is as follows.

- Investigate light-based methods for inspection and validation, including non-invasive, non-contact methods for locating and identifying localized color features created by nanosecond pulsed laser irradiation. (Sub-task 7.1)

*Significant Results and Findings*

Laser speckle was investigated as a method of inspecting and interrogating laser-produced markings. Inspection involved directing polarized, coherent light onto individual color features and capturing the reflected light on a neighboring CCD camera. For this a HeNe laser pointer was utilized and measured, reflected light was specular. The laser – to – sample distance was varied up to ~1.0 m and the sample – to – detector distance was of similar length.

Figure 7 includes a depiction of a six square feature color oxide pattern wherein individual color features were made with a particular accumulated fluence (and laser scan speed). The parallel lines within a feature indicate the associated laser scan directions. A few isolated color islands are also included in this depiction.

The laser scan lines set by hatch between successive passes establishes a rough periodicity that is different than the periodic surface structures produced by femtosecond lasers (described earlier in this document). The periodicity of scan lines shown in Fig. 7 and in Fig. 8 (with a produced multi-feature coating) is of the order ~ 10 μm.

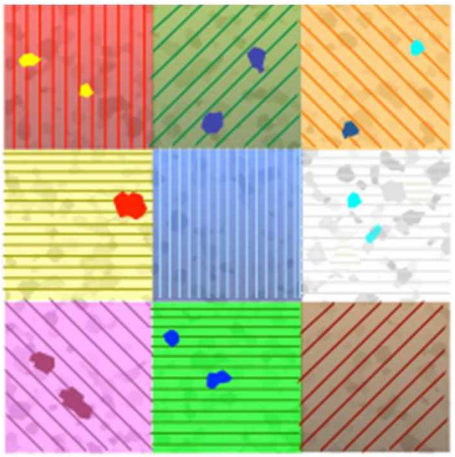

Figure 7: Depiction of a color marking with different color squares. Each square is made by scanning a focused laser beam in a given direction, which is indicated with parallel lines within a colored region. A few areas also show random color islands of unique local color.

As shown in Fig. 8, laser speckle is able to resolve the wavevector of the roughness associated with laser scanning. Sixteen different color features are shown on this particular specimen. The laser speckle patterns obtained from three of these features are included at the top of the figure. Analysis of patterns shows that the semi-major axis of the laser speckle pattern is aligned with the direction of laser scanning (indicated with arrows in the top three patterns).

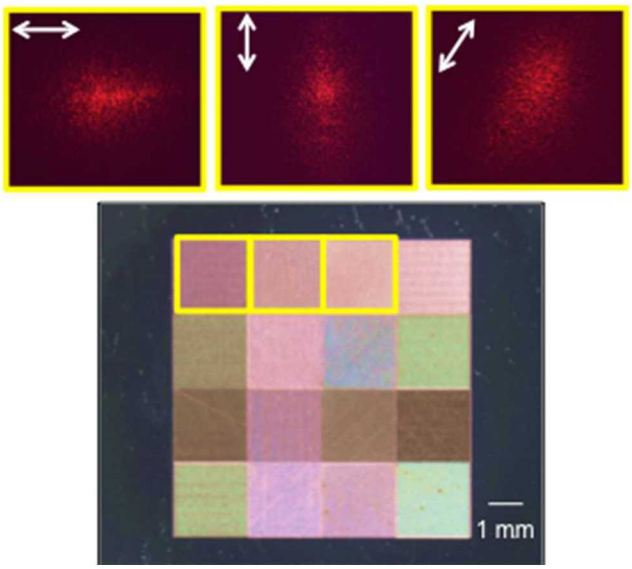


Figure 8. Optical micrograph (bottom image) showing 16 unique color features produced by pulsed laser irradiation at different fluences. In each, the laser scan direction was varied to create a pattern direction that could be probed and detected by laser speckle techniques (akin to the depiction in Fig. 7). The three images shown at the top of the figure were obtained from the three, boxed features below. The arrows indicate the direction of laser scanning, which can be controlled independent of individual color.

With additional experiments, we have initiated research of UV-Vis-IR microspectrophotometry as a method for assessing the local color variations of laser-produced markings on metal and alloy substrates. A commercially available instrument (CRAIC, Inc.) was utilized to examine local color islands produced on stainless steel substrates. The instrument is a modified optical microscope, which allows for rapid assessment of optical properties across a range of visible wavelengths.

An example area interrogated by this method is shown with a plan view optical image in Fig. 9. This image shows two color features with a pink/orange color on the left and a blue/gray average color on the right (with a boundary near the left third of the image). Immersed in these

macroscopic color features are local color islands. Previous work by our team reports on their different colored appearance as evident in an optical microscope.

Attempts to quantify the differences in color of local microscopic features (such as color islands) have involved mapping the spectral response of microscopic regions and spanning large encompassing areas. An example of this is shown in Fig. 10, which plots reflectance for one wavelength (400 nm).

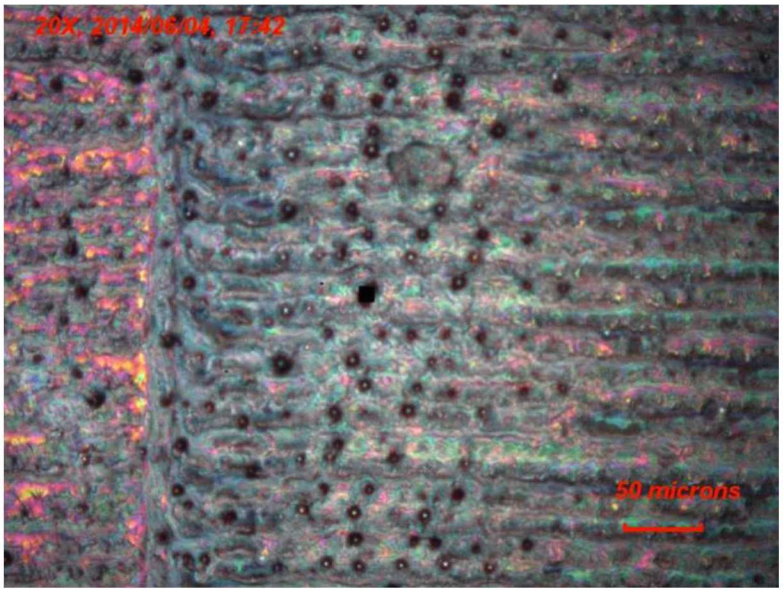


Figure 9. Optical image of an area sampled by UV-Vis-IR microspectrophotometer. This particular area was treated by laser irradiation to form color oxide coatings. Near-circular color islands are evident.

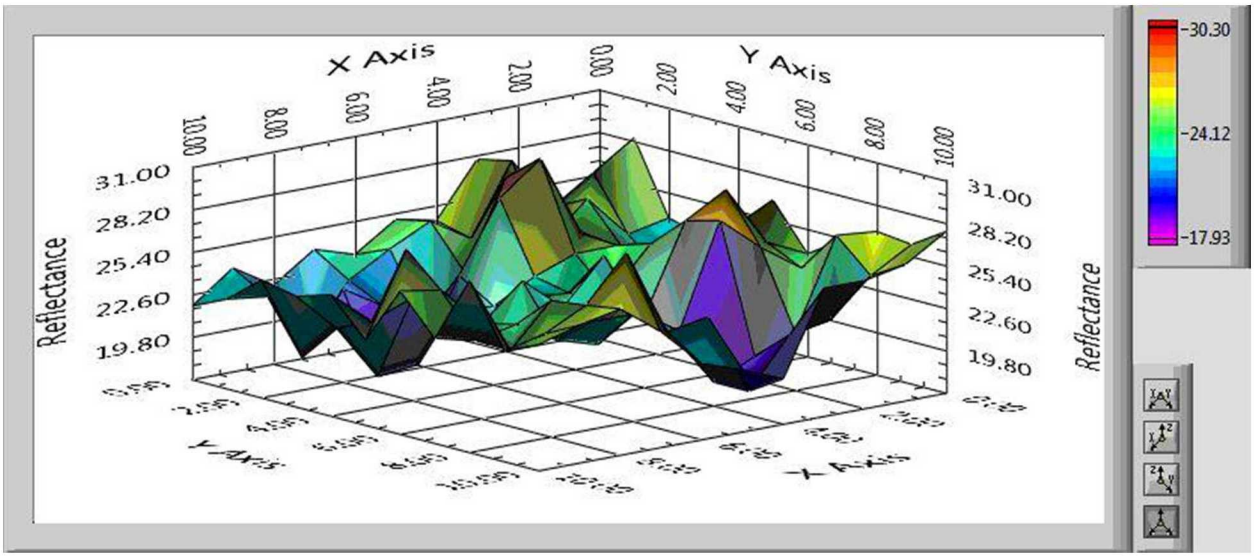


Figure 10. 3D spectral plot of laser fabricated oxide surface with embedded color islands. Results are shown for a single wavelength of inspection (400 nm).

Detailed analysis of reflectance spectra obtained from color islands and neighboring (surrounding) areas of near – constant color were compared to determine if this instrument and approach can resolve the unique optical properties of microscopic features. In Fig. 11, we show that this is feasible. The reflectance values of these two regions are shown for a range of visible wavelengths. The spectra obtained from a color island shows a low average reflectance with a single, broad minima around 510 nm. The spectra obtained from surrounding areas (not including islands) is shown in red to have a larger average reflectance. In addition, the red spectra is characterized by two reflectance minima consistent with higher order interference effects typical of thick oxide coatings. Minima are found at ~ 470 and 590 nm.

Analysis of 3D spectral plots obtained at different wavelengths indicates that color islands can be resolved by this technique. Generally, color islands are characterized by a reduced average reflectance.

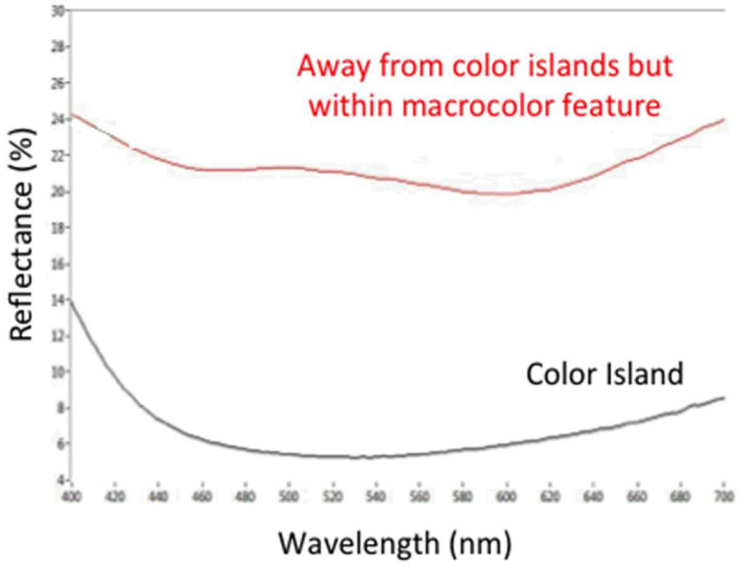


Figure 11. Reflectance spectra taken from a color island (shown in black) and the surrounding areas (shown in red). Note: all areas sampled by microspectrophotometry were treated with the same accumulated laser fluence. The single reflectance minima in the spectra obtained from color islands is consistent with a reduced oxide thickness compared with the thicker oxide coatings of surrounding areas (characterized by multiple reflection minima due to higher order interference effects).

The spectra presented in Fig. 11 are generally consistent with oxide thicknesses measured by scanning electron microscopy. As shown in Fig. 12, the oxide thickness of color islands is thin in comparison to neighboring regions. The thin oxide formed on color islands sits atop a protrusion. Just below this thin oxide coating is a connected metal precipitate that remains attached to the underlying substrate.

Away from the color island, the oxide thickness is nearly ten times thicker, despite receiving an identical laser fluence as islands. The assignments of oxide vs. metal are confirmed by transmission electron microscopy determination of phase and composition.

Investigation of multiple color islands shows similar properties. Oxide coatings on islands are always thinner and are characterized by similar single-minima reflectance spectra.

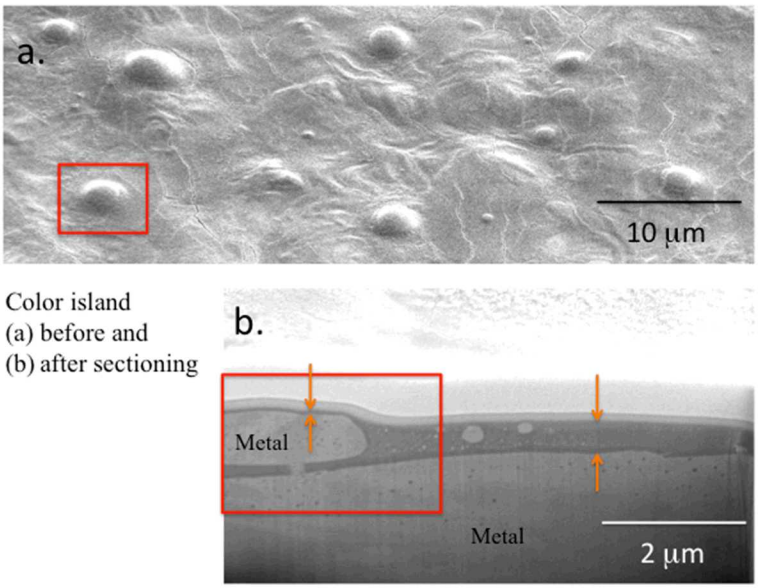


Figure 12. SEM images of color islands before and after focused ion beam sectioning. The bottom image shows the oxide coating in cross section to highlight the differences in oxide layer thickness on top of a color island (inside red box) vs. away from a color island. The dark layer is the oxide produced by laser exposure; its thickness is shown in two different areas by using opposing arrows.

*Key Outcomes*

The key outcomes of this task are as follows.

- Laser speckle analysis has been used to probe laser defined color patterns from up to 1 m working distance, and the wavevector of embedded periodic features has been determined by this method.

- Initial research with a commercially available UV-Vis-IR microspectrophotometer (CRAIC Technologies) has demonstrated an ability to resolve the optical characteristics of micron-sized color islands compared with surrounding areas of different, constant color.

**What opportunities for training and professional development has the project provided?**
*If the research is not intended to provide training and professional development opportunities or there is nothing significant to report during this reporting period, state "Nothing to Report." Describe opportunities for training and professional development provided to anyone who worked on the project or anyone who was involved in the activities supported by the project. "Training" activities are those in which individuals with advanced professional skills and experience assist others in attaining greater proficiency. Training activities may include, for example, courses or one-on-one work with a mentor. "Professional development" activities result in increased knowledge or skill in one's area of expertise and may include workshops, conferences, seminars, study groups, and individual study. Include participation in conferences, workshops, and seminars not listed under major activities.*

Regarding professional development, our graduate student (Samantha Lawrence, Purdue Univ.) and our undergraduate student (Geneva Neiser, New Mexico Tech) were able to attend several technical conferences. Samantha Lawrence attended the International Conference on Metallurgical Coatings and Thin Films (San Diego, CA, April 2014) and the Gordon Conference on Mechanical Properties of Thin Films. Geneva Neiser attended and presented her first poster at the Rio Grande Symposium on Advanced Materials. The primary reason for attending was to present their DTRA-sponsored research. In addition, each student received a top award for their presentation (platform presentation for S. Lawrence and poster presentation for G. Neiser). Additionally, our postdoc, Ryan Murphy, presented his DTRA-funded research at the Surface Analysis 2014 conference. Conference participation was rewarding to each of these three contributors, because they were allowed to interact with peers, experts in the field, and other interested parties.

**How have the results been disseminated to communities of interest?**
*If there is nothing significant to report during this reporting period, state "Nothing to Report." Describe how the results have been disseminated to communities of interest. Include any outreach activities that have been undertaken to reach members of communities who are not usually aware of these research activities, for the purpose of enhancing public understanding and increasing interest in learning and careers in science, technology, and the humanities.*

We have disseminated the results by delivering platform and poster presentations at numerous local and international symposia. The symposia selected for presentation cover a variety of different topics including mechanical property testing, laser technology, corrosion of materials, thin film properties, and light-solid interactions. Presentations included:

1. "Electromechanical and Chemomechanical Performance of Laser Oxide Coatings on Metallic Surfaces" S.K. Lawerence, D.P. Adams, D.F. Bahr, N. Moody, International Conference on Metallurgical Coatings and Thin Films, San Diego, CA, April, 2014.
2. "Ellipsometric Analysis of Laser Fabricated Oxides on Titanium" R.D. Murphy, D.P. Adams, D. Saiz, R.S. Goeke, Surface Analysis 2014, Albuquerque, NM, June, 2014.
3. "Stability of Colored Oxide Films fabricated on Titanium" G. Neiser, D.P. Adams, D. Saiz, R.D. Murphy, M. Rodriguez.

Note: two of these (#'s 1 and 3 above) were awarded best paper or best poster for the conference.

Six publications were accepted, published, or submitted in the past twelve months. Four of these were published in peer-reviewed journal publications and two are currently submitted. These are described below.

1. "Polarization dependent formation of femtosecond laser-induced periodic surface structures near stepped features", R.D. Murphy, B. Torralva, D.P. Adams, S.M. Yalisove, App. Phys. Lett. Vol. 104 (2014) Article #: 231117. *Published*
2. "Nanosecond pulsed laser irradiation of titanium: oxide growth and effects on underlying metal", D.P. Adams, D. Hirschfeld, D.J. Saiz, B. Jared and M.A. Rodriguez, Surface & Coatings Tech. Vol. 248 (2013) p. 38. *Published* (identified as *submitted* in last yrs. report)
3. "Pump probe imaging of laser induced periodic surface structures after ultrafast irradiation of Si", R.D. Murphy, B. Torralva, D.P. Adams, S.M. Yalisove, Appl. Phys. Lett. Vol. 103

(2013) Article #: 141104. *Published* (identified as *submitted* in last year's report)

4. "Mechanical and electromechanical behavior of oxide coatings grown on stainless steel 304L by nanosecond pulsed laser irradiation", S.K. Lawrence, D.P. Adams, N. Moody, D. Bahr, Surface & Coatings Tech. Vol. 235 (2013) p. 860. *Published* (identified as *submitted* in last year's report)
5. "The effects of substrate and film composition on the optical properties of laser grown titanium oxide/oxynitride coatings, R.D. Murphy, D.P. Adams, M.A. Rodriguez, R.S. Goeke, Thin Solid Films, 2014. *Submitted*
6. "Environmental resistance of oxide coatings grown on stainless steel 304L by nanosecond pulsed laser irradiation in air", S.K. Lawrence, D.P. Adams, N. Moody, D. Bahr, Corrosion Science, 2014. *Submitted*

This amounts to 9 peer-reviewed journal articles and 21 presentations over the life of this research project. This has resulted in one Ph.D. degree with two pending (likely to graduate in the next calendar year). In addition, one patent was issued this year. It is US Patent # 8,685,599 titled "A method of pulsed laser intrinsic marking". The authors of this patent are David P. Adams, Joel P. McDonald, V. Carter Hodges, Bradley H. Jared, Deidre Hirschfeld, Dianna S. Blair.

**What do you plan to do during the next reporting period to accomplish the goals?**
*If there are no changes to the agency-approved application or plan for this effort, state "No Change." Describe briefly what you plan to do during the next reporting period to accomplish the goals and objectives.*

During the next year, we plan to complete the following tasks:

**Task 7: Research of microspectrophotometry for inspection and validation of laser color markings**

The awardees shall investigate the reflectance signatures of laser-fabricated color markings using a microspectrophotometer in order to determine the potential of this method for rapid, unambiguous verification of authenticity. We shall start with color oxide patterns produced on stainless steel 304L that are comprised of color islands and surrounding matrix material (of a second, distinguishable color). We will evaluate whether color islands have unique spectral signatures compared to surrounding material. Our work will also determine the minimum size of islands that can be resolved optically with this technique. We will then expand this study to include laser color markings made on other materials.

*Aside: We consider microspectrophotometry a candidate characterization tool for the rapid inspection and validation of laser color markings. This is a commercially available method that provides reproducible measurements over large areas. Our research will investigate its applicability for interrogating microscale color islands that may have a distribution of oxide thickness. A point of this research is to determine the size limitations for reliable measurement.*

**Task 8: Investigate new laser fabrication techniques that produce color markings with improved corrosion resistance**

The awardees shall investigate new methods for fabricating corrosion-resistant color markings. This includes, but is not limited to, color markings made on stainless steel and

titanium alloy. We will start with an investigation of multi-pass laser scan processes for attaining thick, crack-free, color oxide coatings. Experiments will scan a focused laser beam across a specimen at low fluences and repeat this until a desired larger thickness and color are attained. (It is anticipated that this method will avoid large thermal excursions) Additionally, we will investigate de-focused laser beam scanning as a method for growing color oxides to desired thickness and avoid oxide layer cracking. The corrosion resistance of newly produced color features will be evaluated by either salt-water immersion or salt spray exposure tests.

*Aside: Over the course of our study, we have learned that laser color oxide coatings made from metal species contained initially in substrates and oxygen (from air) are well adhered to substrates but may crack, in some cases. These cracks can lead to corrosion attack of the underlying substrate material if subjected to extreme conditions such as submersion in salt water for extended time. However, we have also identified a set of laser process conditions that give rise to crack-free oxides. Generally, this occurs when the laser fluence is kept small. Perhaps this implies that large cooling rates or large changes in temperature lead to cracking. We are proposing to research lower laser fluence processes that implement multiple passes to achieve desired oxide thicknesses (and desired colors). Multiple laser passes will involve a low average fluence per pass. An accumulated number of passes is expected to achieve required oxide thicknesses.*

**Task 9: Research new methods for laser marking curved surfaces**

The awardees shall investigate laser marking of curved surfaces. This will include the creation of color markings as well as periodic ripple topography markings. This should involve the use of a 532 nm or a 1064 nm pulsed laser. The awardees will investigate an expanded set of materials including copper and aluminum. This research will utlize a modified galvo-mirror set that maintains a focused beam across the targeted non-planar surface. We will determine the curvature limits to laser marking of nonplanar surfaces.

*Aside: Our previous research has been limited to planar substrates. We propose to investigate the laser marking of curved surfaces and explore the limitations of this*

*approach. This is important for marking and tagging real-world, 3D objects found in the field. Additionally, we are proposing to expand our set of marked materials to include Cu and Al, which should be treated with a 532 nm laser (instead of our past 1064 nm wavelength laser). Limits to this approach will be explored, by working with specimens of different curvature. Our approach will involve maintaining a focused beam across a pre-mapped surface. Both color markings and topographical (rippled) markings should be explored.*

**Task 10: Complete model simulations of laser-induced ripple formation – involves an ElectroMagnetic field solver**

The awardees shall investigate the complex light-solid interactions that give rise to periodic ripple topography on a surface when irradiated by a laser. Specifically, the University of Michigan student will team with Sandia National Laboratories' staff to evaluate the fundamental mechanisms giving rise to periodic topography. This should involve a numerical modeling approach (COMSOL). We will investigate the relative roles of light polarization, surface plasmon polaritons, and Fresnel diffraction on forming periodic surface features. The awardees should predict the characteristic wavelength and orientation (i.e., wavevector) of surface ripples. Tests in the laboratory will validate model predictions.

*Aside: This task involves the basic research of fundamental light-solid interactions that give rise to periodic ripple topography at surfaces. In previous years of this program, we have completed a number of experiments that determine the timescales involved with ripple formation and identify the effects of initial surface topography. The proposed task will include various pulsed laser light – solid interactions in an attempt to develop a complete understanding of what gives rise to periodic surface ripple markings. Our numerical modeling approach will implement COMSOL – code that was bought during the past year of research. This will be used specifically to investigate the competing effects of surface plasmon polaritons and Fresnel diffraction on ripple formation. We expect to publish these results in a High Index factor journal.*

UNCLASSIFIED

# Basic Research of Intrinsic, Tamper Indication Markings Defined by Pulsed Laser Irradiation, David P. Adams, Sandia Labs, IACRO 13-5897I

Sandia National Laboratories

**Objective:** We will research how short (ns) and ultra-short (fs) laser pulses interact with the surfaces of various materials to create complex color layers and morphological patterns.

**Method:** We are investigating the site-specific, formation of microcolor features. Also, research includes a fundamental study of the physics underlying periodic ripple formation during femtosecond laser irradiation.

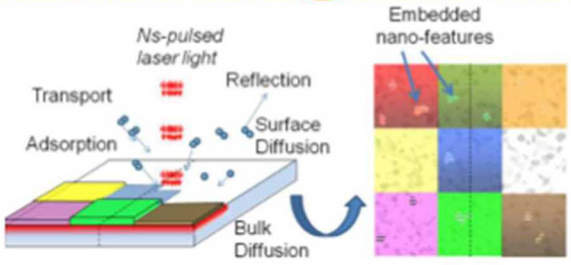


**Status of effort:** Laser induced color markings and ripple patterns have been demonstrated on an increased number of materials. The stability of laser-defined color markings was investigated for corrosion resistance in salt fog, spray and immersion. Electromagnetic modeling has investigated light-solid interactions leading to periodic surface patterns.

**Personnel Supported:** 2 Technical Staff, 2 Professors, 2 Students, 1 Postdoc, 1 Technician

**Publications & Meetings:** 4 Published Papers, 2 Submitted Papers, 3 Conference Presentations, 2 Best Paper/Poster Awards, 1 Granted Patent in past 12 months

**Goals/Milestones**

- Research corrosion resistance of oxide color markings (salt spray, fog and immersion tests)
- Investigate role of surface plasmon polaritons on rippled surface patterns defined via laser exposure
- Through modeling, investigate effects of multi-source scattering and interference on ripple patterns
- Initiated research of color feature interrogation involving microspectrophotometry and speckle

**Funding Profile**

$349k FY11 $350k FY12 $350k FY13 $350k FY14

**Contact information**

David P. Adams dpadams@sandia.gov 505-844-8317
Neville Moody, nrmoody@sandia.gov 925-294-2622
Cole Yarrington, cdyarri@sandia.gov 505-844-3734

Sandia is a multi-program laboratory managed and operated by Sandia Corporation, a wholly owned subsidiary of Lockheed Martin Company, for the United States Department of Energy's National Nuclear Security Administration under Contract DE-AC04-94AL85000.

Cleared for Public Release